Key Points:

- High-Energy Particle Detector (HEPD-01) measurements of solar protons (50–250 MeV) emitted during the first ground-level enhancement of solar cycle 25
- Spectral analysis conducted on a energy-extended, time-integrated proton spectrum using also ACE, ERNE, and EPHIN data
- Time-of-arrival analysis in good agreement with the literature and highlights the central role of HEPD-01 at energies around hundreds of MeV

Correspondence to:

M. Martucci,
matteo.martucci@roma2.infn.it

AGU ADVANCING EARTH AND SPACE SCIENCE

The First Ground-Level Enhancement of Solar Cycle 25 as Seen by the High-Energy Particle Detector (HEPD-01) on Board the CSES-01 Satellite

Matteo Martucci[1,2], Monica Laurenza[3], Simone Benella[3], Francesco Berrilli[2], Dario Del Moro[2], Luca Giovannelli[2], Alexandra Parmentier[1,3], Mirko Piersanti[4], Gabor Albrecht[5,6], Simona Bartocci[1], Roberto Battiston[5,6], William J. Burger[6,7], Donatella Campana[8], Luca Carfora[1,2], Giuseppe Consolini[3], Livio Conti[1,9], Andrea Contin[10,11], Cinzia De Donato[1], Cristian De Santis[1], Francesco Maria Follega[5,6], Roberto Iuppa[5,6], Alessandro Lega[5,6], Nadir Marcelli[1,2], Giuseppe Masciantonio[1], Matteo Mergé[1,12], Marco Mese[8,13], Alberto Oliva[11], Giuseppe Osteria[8], Francesco Palma[1,2], Beatrice Panico[8], Francesco Perfetto[8], Piergiorgio Picozza[1,2], Michele Pozzato[11], Ester Ricci[5,6], Marco Ricci[14], Sergio Bruno Ricciarini[15], Zouleikha Sahnoun[11], Valentina Scotti[8,13], Alessandro Sotgiu[1,2], Roberta Sparvoli[1,2], Vincenzo Vitale[1], Simona Zoffoli[16], and Paolo Zuccon[5,6]

[1]INFN, Sezione di Rome "Tor Vergata", Rome, Italy, [2]Department of Physics, University of Rome "Tor Vergata", Rome, Italy, [3]INAF-IAPS, Rome, Italy, [4]Department of Physical and Chemical Sciences, University of L'Aquila, L'Aquila, Italy, [5]University of Trento, Trento, Italy, [6]INFN-TIFPA, Trento, Italy, [7]Centro Fermi, Rome, Italy, [8]INFN-Sezione di Napoli, V. Cintia, Naples, Italy, [9]Uninettuno University, Rome, Italy, [10]University of Bologna, Bologna, Italy, [11]INFN-Sezione di Bologna, Bologna, Italy, [12]Now at ASI Space Science Data Center (SSDC), Rome, Italy, [13]University of Naples "Federico II", Naples, Italy, [14]INFN-LNF, Rome, Italy, [15]IFAC-CNR, Florence, Italy, [16]Italian Space Agency, Rome, Italy

Abstract In this work we present the High-Energy Particle Detector (HEPD-01) observations of proton fluxes from space during the 28 October 2021 solar energetic particle event, which produced a ground-level enhancement on Earth. The event was associated with the major, long-duration X1-class flare and the concomitant coronal mass ejection (CME) that erupted from the Active Region 12887. This is the first direct measurement from space of solar particles emitted during the current solar cycle, recorded by a single instrument in the energy range from ∼50 MeV/n up to ∼250 MeV/n. We have performed a Weibull-modeled spectral analysis of the energy spectrum in the wide energy range 300 keV–250 MeV, obtained from combination of HEPD-01 proton measurements with the ones from ACE/ULEIS, SOHO/EPHIN, and SOHO/ERNE. The good agreement between data and model, also corroborated by a comparison with other spectral shapes commonly used in these studies, suggests that particles could have possibly been accelerated out from the ambient corona through the contribution of stochastic acceleration at the CME-driven shock, even if the presence of seed populations influencing spectral shape could not be excluded. Finally, a Solar Proton Release time of 16:01 UTC ± 13 min and a magnetic path-length of $L = 1.32 \pm 0.24$ AU have been obtained, in agreement with previous results for this event. We remark that new and precise data on protons in the tens/hundreds MeV energy range—like the one provided by HEPD-01—could shed more light on particle acceleration as well as provide a reliable parametrization of solar energetic particle spectra for Space Weather purposes.

Plain Language Summary In this work we present the observation from space of protons emitted by the Sun during the 28 October 2021 solar event. This event was particularly strong and it was even registered at Earth by instruments called Neutron Monitors. Such highly energetic phenomena are rather rare and they can give a lot of information on particle acceleration and propagation from Sun to Earth. By using data from various spacecrafts, like High-Energy Particle Detector, we were able to address some characteristics of this event, like its duration, the most probable mechanism that accelerate particles, the path traveled by such particles, as well as to constrain the time in which they are accelerated.

1. Introduction

After decades of studies, it is now generally accepted that solar energetic particles (SEPs) are accelerated by both flares and shocks driven by coronal mass ejections (CMEs). SEPs can be classified into impulsive and gradual events (Cane et al., 1986; Cliver et al., 1982; Desai & Giacalone, 2016; Kahler et al., 1978, 1984), based on their

Cinzia De Donato, Francesco Maria Follega, Alessandro Lega, Giuseppe Masciantonio, Alberto Oliva, Francesco Palma, Beatrice Panico, Michele Pozzato, Sergio Bruno Ricciarini, Zouleikha Sahnoun, Valentina Scotti, Alessandro Sotgiu, Vincenzo Vitale

Supervision: Roberto Battiston, Roberto Iuppa

Validation: Gabor Albrecht, Giuseppe Consolini, Livio Conti, Nadir Marcelli, Matteo Mergé, Marco Mese, Ester Ricci, Marco Ricci, Sergio Bruno Ricciarini, Zouleikha Sahnoun, Alessandro Sotgiu

Writing – original draft: Matteo Martucci

Writing – review & editing: Monica Laurenza, Simone Benella, Francesco Berrilli, Dario Del Moro, Luca Giovannelli, Alexandra Parmentier, Mirko Piersanti

properties, composition and source. The former ones are generally much less intense and associated with both short-duration soft X-ray emission from low altitudes of the flare site (Pallavicini et al., 1977) and fast-drift type III radio emission (Wild et al., 1963). Furthermore, impulsive events are thought to be a result of flare acceleration (Aschwanden, 2002) and typically present an enrichment in ^{3}He and heavy ions such as Fe (Mewaldt et al., 2012; Tylka et al., 2005). In contrast, gradual events are associated with type II radio emission and they are believed to be accelerated in the corona by CME-driven shocks (Reames, 1999), producing the highest intensities among SEP events. Hybrid events are possible, mixing up characteristics from impulsive and gradual ones (Cane et al., 2010; Cliver, 1996; Gopalswamy et al., 2012). Recent studies have made it possible to gain further insights into the origin, acceleration, and propagation of SEPs: see, for example, Dayeh et al. (2009), Kahler et al. (2017), Mewaldt et al. (2012), Tylka et al. (2005, 2010), Rouillard et al. (2011, 2016), Kollhoff et al. (2021), and Frassati et al. (2022). Nevertheless, the contribution and relative weights of flare and shock acceleration are still under debate (e.g., Cane et al., 2006; Tylka et al., 2005). An extensive review on the topic can be found in Desai and Giacalone (2016), Zhang et al. (2021). The understanding of particle acceleration is even more challenging for the most energetic SEP events—generally >500 MeV. Such events generate showers in the terrestrial atmosphere whose secondary products can be detected by the network of ground-based neutron monitors (NMs) (Poluianov et al., 2017); these are the ground-level enhancements (GLEs). GLEs are rather rare—only 73 have been recorded since 1940s (Vainio et al., 2017), the last one being the event under study. GLEs time-profiles are usually characterized by two components: a rapid onset, marking an impulsive injection of particles, which poses temporal constraints to any putative acceleration process (Moraal & McCracken, 2012; McCracken et al., 2008; Vashenyuk et al., 2006, 2011) and a gradual phase that can be attributed to shock mechanisms (Kahler et al., 2012; Nitta et al., 2012) or to stochastic acceleration due to the local turbulence and/or the turbulence generated by the plasma expansion behind the shock wave (Pérez-Peraza et al., 2018; Reames, 1999; Rouillard et al., 2011). Thus, the mechanisms of particle production and acceleration leading to GLEs has not reached a general consensus and other scenarios have been suggested (Bieber et al., 2002; Gopalswamy et al., 2018; Kahler et al., 2017; Kouloumvakos et al., 2020; Zhang et al., 2021; Zhao et al., 2018). It has also been proposed that—beside the acceleration by CMEs via diffusive-shock acceleration (DSA)—stochastic re-acceleration of energetic protons might be important, for example, by means of enhanced Alfvénic turbulence in the downstream region of a shock wave (Afanasiev et al., 2014, 2018), even if this does not explain the two components observed in GLE events.

All the acceleration processes leave various distinct signatures in the differential energy spectrum, thus providing crucial constraints on the origin of SEPs. It is important to notice that the observed spectral features of an event could arise from different solar locations as to particle acceleration, for example, the flare region, corona, or even the interplanetary space, and/or different mechanisms; for this reason, the overall shape of a solar particle spectrum may exhibit a combination of signatures, linked to different processes, usually complex to disentangle, like the transport of energetic particles inside the interplanetary space (Zhao & Zhang, 2016). Moreover, the transport itself is still a matter of study, with recent advances regarding the role and the efficiency of propagation perpendicular to the mean magnetic field, resulting in a wide spreading of SEPs (Dresing et al., 2012; Dröge et al., 2016; Laitinen et al., 2016; Richardson et al., 2014).

The study of GLE spectra is of particular scientific interest because the acceleration processes in such cases are very efficient (Mewaldt et al., 2012) and the high-energy solar particles can reach the Earth at 1 AU with minimal disturbances due to scattering (Cliver et al., 1982). Thus, the differential spectrum of protons during GLEs can provide crucial information on SEP origin, acceleration and transport. The most common theory to explain such events involves the diffusive-shock acceleration (Gordon et al., 1999; Lee, 1983), predicting a power law spectrum with an expected roll-over at high energies, due to the energy dependence of the diffusion coefficient (Ellison & Ramaty, 1985). Moreover, high-energy SEPs/GLEs are important in the framework of Space Weather, as they pose the greatest hazard for spacecraft and instruments, as well as aircraft and also human crews. In particular, proton spectra can be used to characterize the particle radiation environment around the Earth (Grimani et al., 2012; Laurenza et al., 2019) and estimate the resulting absorbed dose (Berrilli et al., 2014; Brueckner et al., 1995)—which is crucial for manned space missions. In addition, they allow to assess the possible effects of solar particles on the molecules of the atmosphere (Damiani et al., 2008; Jackman et al., 2005). The high-energy portion of such spectra have been found to severely impact various components of spacecraft, starting from the electronics. SEPs could also effect signal propagation between Earth and satellites due to Polar Cap Absorption (PCA) which results from intense ionization of the D-layer of the polar ionosphere (Zhang et al., 2021).
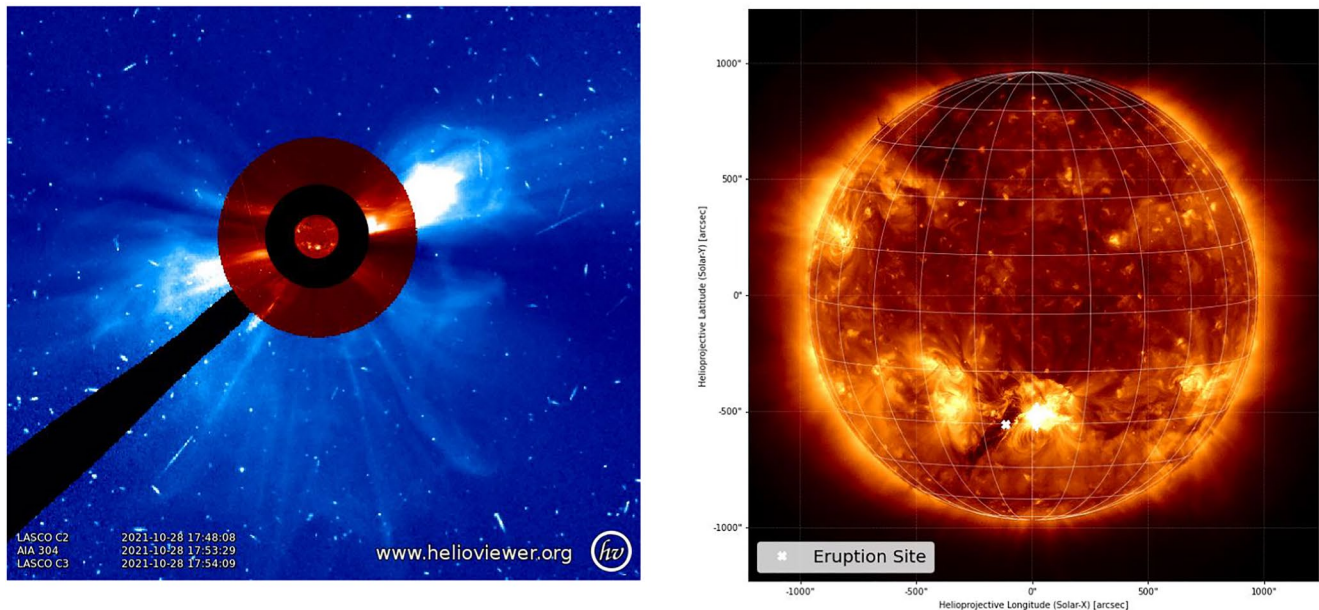
Figure 1. Left panel: composite image of the Sun, created with the Atmospheric Imaging Assembly (AIA) 304, LASCO C2 and C3 images approximately 2 hr after the launch of the coronal mass ejection. Right panel: AIA 193 Full disk image of the Sun, approximately at the time of the filament eruption. The white cross marks the position of the erupting filament that appears as a dark structure on the lighter background.

In this work, we have analyzed proton data obtained by the High-Energy Particle Detector (HEPD-01) during the SEP/GLE event of 28 October 2021. Thanks to its proven observational capabilities, HEPD-01 can give accurate and robust SEP measurements in the high-energy portion of the spectrum (up to 250 MeV), bridging the gap between low-energy measurements by in-situ spacecraft (like ACE) and the ones from NMs on ground at ∼GeV energies.

HEPD-01 data, together with the information gained from other spacecrafts (ACE/ULEIS, SOHO/EPHIN and SOHO/ERNE), have allowed us to obtain an energy-extended event-integrated proton spectrum from 300 keV to ∼250 MeV. We have also fitted this spectrum using a Weibull distribution, which has been found to be the best fit for gradual SEP events (Laurenza et al., 2015) and can be associated with shock acceleration (Pallocchia et al., 2017). Moreover, we have performed an analysis on the times of arrival of protons at different energies. Finally we have drawn conclusions about the new insights attained by our study about the origin and propagation of protons from the Sun to Earth.

2. The SEP Event of 28 October 2021

The solar event associated with the SEP under analysis, occurred on 28 October 2021, at approximately at 15:15 UTC in the lower coronal layers. A Full-Halo CME was well imaged by SOHO/LASCO (Brueckner et al., 1995; Domingo et al., 1995) as represented in Figure 1 (left panel). This fast (estimated radial velocity ∼1,260 km/s), asymmetric Halo CME was observed in LASCO C2 imagery at 15:48 UTC, at approximately the same time when a type II radio emission—typically marking the formation of a CME shock—and a type IV radio emission were registered. The most probable source for the CME itself was a filament eruption observed on 28 October 2021 at $t_0 = 15:15$ UTC in the southern solar hemisphere (white cross in Figure 1, right panel). The filament ejection was recorded by SDO/AIA (Lemen et al., 2012; Pesnell et al., 2011) imagers. The filament erupted from the neighborhood of Active Region (AR) 12887, which, at the moment of the expulsion, was close to the disk's lower center and directly facing Earth (W02S26); this suggests a non-perfect magnetic connectivity, even more so because the associated SEP event lasted about 6 days. This AR was particularly active, emitting a series of C- and M-class flares and culminating in a major, long-duration X1.0-class solar flare at 15:35 UTC (started at 15:17 and ended at 15:48 UTC), either triggered by or triggering the filament eruption (Georgoulis et al., 2019).
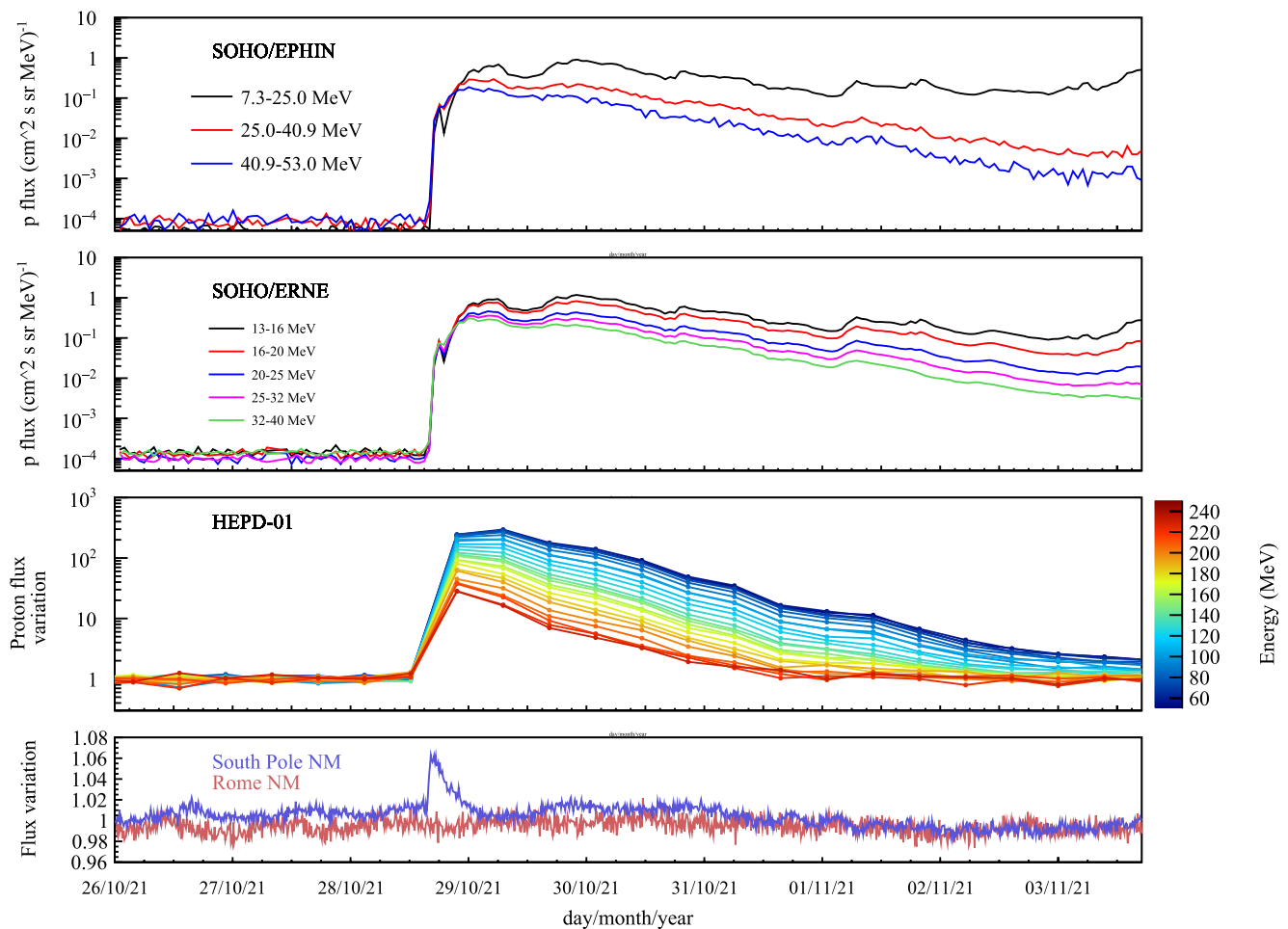
Figure 2. Time evolution of the 2021 October solar energetic particle event, as seen by EPHIN and ERNE (first two panels)—both located on the SOHO spacecraft placed in the Lagrangian Point L1—in 3 and 5 energy intervals, respectively. The passage of the shock is evident in both the time-profiles. A >300x variation of ~50 MeV proton fluxes was registered by the High-Energy Particle Detector at Low-Earth Orbit (third panel). Finally, time-profiles of two Neutron Monitors on ground (South Pole and Rome) are shown in the fourth panel.

The association of the CME with the filament expulsion is straightforward, given the CME characteristics (full-halo CME, slightly displaced toward the South of the ecliptic) and the filament position on the disk (white cross in right panel of Figure 1). The images, acquired by the COR2 instrument onboard STEREO-A, corroborate this interpretation, confirming that part of the CME was ejected directly toward the Earth. The high efficiency of the eruption in accelerating energetic particles, likely in the strong CME-driven coronal shock wave, and the favorable position of the CME source help explain the signature of a GLE detected minutes later by the Neutron Monitor network (Mavromichalaki et al., 2011). Indeed, several NMs detected an increase in count rates from around 16:00 UT on 28 October 2021 just until next midnight, as reported in the official database of Neutron Monitor count rates during GLEs at: https://gle.oulu.fi/. The GLE#73 is therefore the first GLE event of Solar Cycle 25 (SC-25). The appearance of a GLE event at the beginning of SC-25 might indicate that, after a minimum quite similar to the one before SC-24, an unexpected sudden increase in solar activity starting in late 2020 is present (Jain et al., 2021) and that the amplitude of this Solar Cycle may be higher than SC-24 (Diego & Laurenza, 2021; Penza et al., 2021).

Figure 2 (first two panels) shows the temporal profile of the SEP event up to about 50 MeV, as seen by EPHIN (Müller-Mellin et al., 1995) and ERNE (Torsti et al., 1991)—both mounted on the SOHO spacecraft at Lagrangian Point L1—in three and five energy intervals, respectively. An overall ~300x variation of ~50 MeV proton fluxes, due to the injection of solar protons, was registered by HEPD-01 (at Low-Earth Orbit), as can be seen from the third panel of Figure 2. The increase was not only limited to low-energy particles, but it involved also protons

with energies >200 MeV. The onset of the SEP appears to be rapid, with a gradual fall to undisturbed levels in ∼6 days for the low-energy protons. Finally, data from two Neutron Monitors on ground (South Pole and Rome) are shown in the fourth panel of Figure 2. Due to its location at high latitudes (low cutoff rigidity), the South Pole NM shows the signature of a GLE, whereas the Rome NM (located at ∼40°N of latitude) did not record any increase (high cutoff rigidity). As a matter of fact, the GLE#73 extended to rigidity of about 2 GV ∼1.26 GeV.

3. Limadou Mission and High-Energy Particle Detector

The CSES-01 satellite (Shen et al., 2018) was launched on 2 February 2018, and is currently flying on a sun-synchronous polar orbit at a ∼507 km altitude, with a 5-day revisiting periodicity. It is the first of a series of multi-instrument satellites, scheduled for launch in a few years, mainly dedicated to the monitoring of the electromagnetic field, plasma and particle perturbations in the ionosphere and magnetosphere, either due to natural sources, like earthquakes or solar events, or artificial emitters. Despite the fact that all payloads on board the satellite are switched-off at latitude below −70° and above +70°, the orbital characteristics of CSES-01 allow for a detailed investigation of the high-latitude regions of the Earth—the ones more sensitive to the influence of the Sun. HEPD-01 is one of the nine instruments on board the satellite; it was designed and built in the framework of the CSES/Limadou project by the Italian branch of the CSES Italian-Chinese collaboration. It is a light and compact payload (40.36 × 53.00 × 38.15 cm, total mass ∼45 kg), made up of a series of sub-detectors: from the top of the detector, two double-sided silicon microstrips planes (213.2 × 214.8 × 0.3 mm) providing tracking information, a layer of plastic segmented scintillator (6 paddles, 20 × 3 × 0.5 cm each), a range calorimeter for energy measurement, composed of a stack (TOWER) of 16 plastic scintillators, $P_1…P_{16}$ (15 × 15 × 1 cm), and, finally, a 3 × 3 matrix of Lutetium-Yttrium Oxyorthosilicate (LYSO) inorganic scintillator crystals (5 × 5 × 4 cm). The instrument is surrounded—laterally and at the bottom—by 5 plastic scintillators which reject particles that do not deposit all their energy inside the detector (VETO). The trigger system comprises the stripped scintillator, to recognize multiple events, and the first and second plane of the calorimeter. The detector is optimized to measure electrons in the 3–100 MeV energy range, and protons between 40 and 250 MeV, as well as light nuclei. The HEPD-01 capabilities for galactic and trapped protons and Space Weather studies have already been assessed in Bartocci et al. (2020), Martucci et al. (2022), Palma et al. (2021) and in Piersanti et al. (2022). More technical details on the instrument itself can be found in Picozza et al. (2019), Ambrosi et al. (2020), Sotgiu et al. (2020), and Ambrosi et al. (2021).

4. HEPD-01 Proton Data

The selection of protons in HEPD-01 is described in detail in Bartocci et al. (2020). In order to give a valid trigger to start the data acquisition process, a proton must cross a single paddle of the trigger plane (to avoid multi-particle events and reduce secondaries) and at least the first two planes of the upper calorimeter, P_1 and P_2. Even under high particle rates expected during SEP events or crossing of the South Atlantic Anomaly, no major issues of saturation have been observed. After a valid trigger is acquired, only protons fully contained (e.g., those that stop inside the TOWER + LYSO sub-detector) are included in the final flux sample, while particles generating signal in one of the VETO planes are discarded to guarantee that all the energy of the primary particle is deposited inside the instrument. The discrimination between protons and other particle populations is performed using the P_1 signal distribution as a function of the total energy released inside the TOWER + LYSO sub-detector, as shown in Figure 2 of Bartocci et al. (2020). Other auxiliary selections are required to further clean the sample. The same selections are also applied to a dedicated GEANT4 MonteCarlo simulation to estimate the geometrical factor, see Figure 4 of Bartocci et al. (2020). Selection efficiencies are obtained through dedicated simulations as well and calibrated—where possible—with in-flight data. For what concerns the systematic uncertainties, we used the same approach employed in Bartocci et al. (2020): such systematics as a function of energy can be found in Figure 5 of that paper. Regarding the geomagnetic selection applied to discriminate between protons coming from outside the magnetosphere and the under-cutoff re-entrant albedo populations, we made use of a rigidity cutoff map obtained using a dedicated simulation with the Tsyganenko 96 magnetospheric model (Tsyganenko, 1995) and with the external magnetic field input parameters corresponding to the period of the SEP event. A parallel approach was implemented using the AACGM (Altitude-Adjusted Corrected Geomagnetic) coordinates reference frame (Stephens et al., 2017). In this way, we corrected the estimation of the McIlwain parameter L—hereafter L shell—obtained through the International Geomagnetic Field Reference (IGRF)
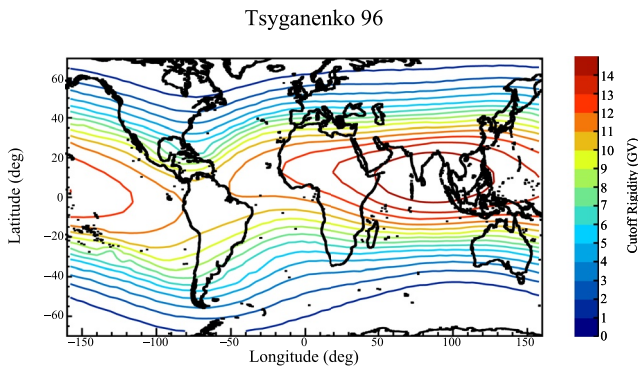
Figure 3. Map of the distribution of the cutoff rigidities as a function of geographic longitude and latitude, obtained using a dedicated simulation with the Tsyganenko 96 magnetospheric model.

model (Erwan et al., 2015). In this latter case, we selected only portions of the CSES-01 orbit that were above a value of the L-parameter greater than 7, to assure that all coming protons with energy >50 MeV were of cosmic origin (i.e., above the cutoff threshold). Of course, the same geomagnetic selection was applied to the estimation of the Live Time of the instrument for consistency purposes. This approach—together with the tilt in the geomagnetic field and the fact that all payloads are switched-off at ∼70° of latitude—resulted in HEPD-01 being able to detect solar and galactic particles with sufficient statistics only near the polar caps. The two methods are found to be in very good agreement at >50° latitudes where HEPD-01 data are considered in this study. Therefore, the proton rigidities selected with the Tsyganenko 96 map coincide—inside the systematic uncertainties—with the protons selected using the L shell map; the former is shown in Figure 3.

5. SEP Spectral Analysis

The evolution of the proton energy spectrum of a SEP event—particularly during the early hours—is useful to assess the event energy content. Using HEPD-01 proton data we have been able to extract 30-min differential proton spectra during the first 24 hr of the event—see Figure 4 (left panel)—between 50 and 250 MeV. A fit with a simple power-law shows that the spectral index γ of the event in this energy range gradually rises from 1.12 ± 0.49 to 2.47 ± 0.38—see right panel. Although the errors associated with the fit parameters are quite large, it is possible to observe a softening of the spectral index over time.

One of the main focus of this analysis, however, is to obtain a event-integrated extended-energy spectrum; to do so, we need to consider not only HEPD-01 proton data, but also data from other experiments in orbit, including ACE/ULEIS (Mason et al., 1998), SOHO/EPHIN (Müller-Mellin et al., 1995) and SOHO/ERNE (Torsti et al., 1991) (all accessible from the OMNIWEB website at https://omniweb.gsfc.nasa.gov/ftpbrowser/flux_spectr_m1.html). The total event-integrated spectrum is calculated by summing up the SEP intensities measured in each energy bin over the event duration, which is chosen to go from 28 October (18:00 UTC) to 3 November (18:00 UTC), when all the energy channels of the various instruments detected some signature of solar injection with respect to the background; this technique has already been employed in Bruno et al. (2019). In this way, we could construct a spectrum of protons as a function of energy, from ∼300 keV to ∼250 MeV, notably increasing the information to be inferred. Moreover, since the lowest energy channels of ACE/ULEIS are affected by electron contamination (Bruno et al., 2019) and the high-energy channels of SOHO/ERNE are affected by
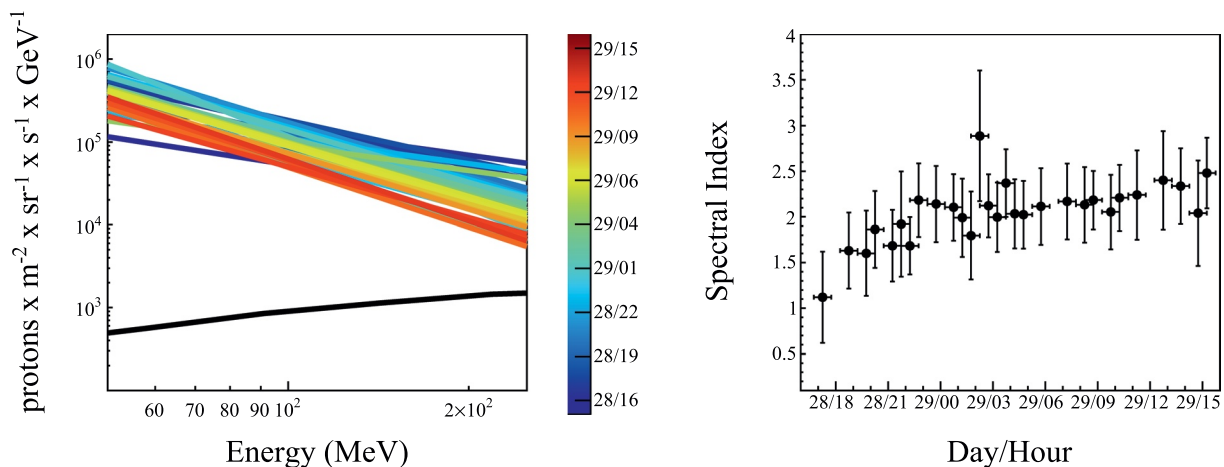
Figure 4. Left panel: High-Energy Particle Detector 30-min solar energetic particles (SEP) proton fluxes as a function of energy for the days of 28 and 29 October (see color bar on the right). The galactic cosmic-ray (GCR) spectrum—obtained during the 7 days before the start of the SEP—is reported as a comparison (black curve). Right panel: time evolution of the spectral index γ. The vertical error bars account for the parameter uncertainties of the fit performed on the single SEP spectra.

Oct. 28 (1800 UTC) - Nov. 3 (1800 UTC)
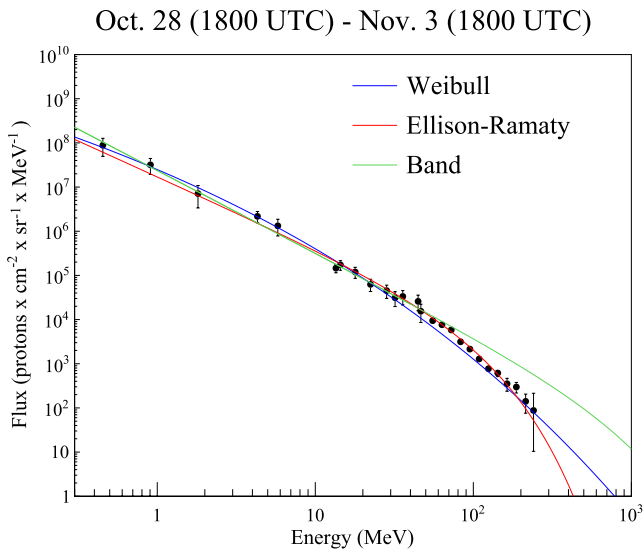
Figure 5. The pure, energy-extended event-integrated solar proton spectrum obtained by combining the observations of the High-Energy Particle Detector with the ones from ACE, SOHO/EPHIN, and SOHO/ERNE. The vertical error bars account for both statistical and systematic uncertainties, plus the 20% added to account for other uncertainties. The blue, red and green curves represent the fit performed by using the Weibull, Ellison-Ramaty and Band functions respectively.

saturation (Miteva et al., 2020), only >300 keV and <80 MeV intensities, respectively, have been considered in the analysis for these two experiments. Nevertheless, the spectral fitting procedure is usually valid if performed on a pure solar spectrum, while our spectrum is still a sum of solar and galactic contributions. A further step is estimating the background spectrum that will be subtracted from this total proton flux. The removal of this background, due to galactic cosmic-ray (GCR) protons, is a delicate issue. Commonly, to account for short-time variations, the time-dependent GCR background component is computed for defined time-intervals, by extrapolating to lower energies the fit of the measured spectrum performed above the maximum SEP energy (Bruno et al., 2018). In the present study, for statistical reason, a single GCR proton spectrum has been calculated, specifically the one spanning the quiet period from 20 October to 27 October. As a matter of fact, no solar flares or CMEs during such period were strong enough to cause disturbance in the population of MeV protons; for this reason, our background can be considered as stable. Having constructed both total and background proton energy spectra, the final, pure solar flux—integrated over the duration of the SEP—is obtained by applying a simple bin-by-bin background subtraction, that is, subtracting for each energy bin the value of the GCR protons collected during the 7-day interval prior to the SEP event. A 20% uncertainty on each data point has been considered a safe assumption to take into account measurements acquired from different instruments and systematic errors due to the subtraction. The final, pure, energy-extended event-integrated solar proton spectrum is depicted in Figure 5. In total, we used 4 energy channels for ACE (320 keV–7.2 MeV), 8 channels for ERNE (13–80 MeV), 4 channels for EPHIN (4–53 MeV) and 12 channels for HEPD-01 (50–250 MeV).

In order to have a reliable parametrization of the spectrum and get some information about the SEP acceleration sources, we have fitted the event-integrated proton energy spectrum with a Weibull distribution (Frisch & Sornette, 1997; Kim et al., 2007; Laurenza et al., 2013, 2015; Xapsos et al., 2000)—also known as the two-parameter stretched exponential. It has been suggested in Laurenza et al. (2016); Pallocchia et al. (2017) that such distribution can be associated with particle acceleration by *killed* stochastic processes exhibiting power-law growth in time of the velocity expectation, such as the classical Fermi process, or shock-surfing acceleration.

The corresponding function has the form:

$$\frac{dJ}{dE} = A\left(\frac{E}{E_0}\right)^{b-1} \sqrt{E} \; e^{-\left(\frac{E}{E_0}\right)^b} \tag{1}$$

where b is a spectral index, E_0 is a characteristic energy and A is a scaling factor, as discussed in Pallocchia et al. (2017). The spectral features have been found to be consistent with this Weibull-like shape, over the whole duration of the event. For comparison, we have also fitted the same spectrum using both Band and Ellison-Ramaty functions. Their mathematical representation is the following:

$$\phi_{Band}(E) = \begin{cases} AE^{\gamma_a} e^{-\frac{E}{E_0}}, \\ AE^{\gamma_b}[(\gamma_b - \gamma_a)E_0]^{(\gamma_b - \gamma_a)} e^{(\gamma_a - \gamma_b)} \end{cases} \tag{2}$$

and

$$\phi_{Ellison\text{-}Ramaty}(E) = AE^{\gamma} e^{-\frac{E}{E_R}}, \tag{3}$$

More information on the meaning of these functions, their derivation and their parameters can be found in Band et al. (1993) and in Ellison & Ramaty (1985), respectively. The resulting, reduced χ^2 is 0.48 for the Weibull, 0.94 for the Band and 1.12 for the Ellison-Ramaty. The event-integrated spectrum together with the aforementioned
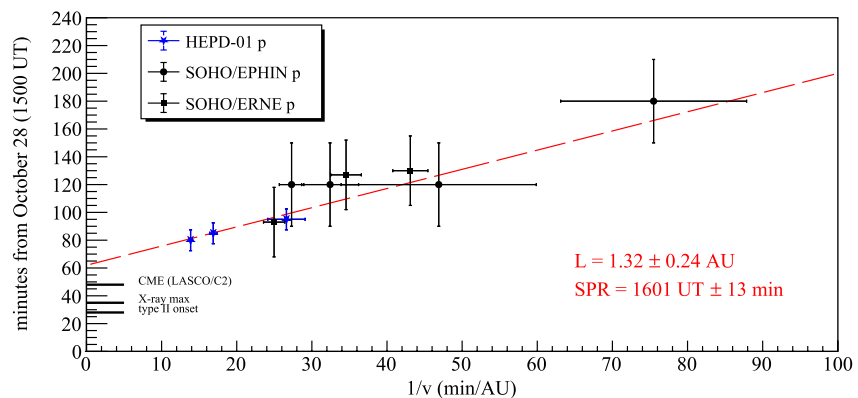
Figure 6. Onset time of the October 28 solar event versus 1/velocity, using the High-Energy Particle Detector (HEPD-01), EPHIN and ERNE proton data. The red dashed line represents the fit to the experimental points, while the short horizontal lines on the *y*-axis indicate the onset of the type II radio emission, the maximum of the X-ray emission and the first observation of the coronal mass ejection by LASCO/C2. The path-length L and Solar Proton Release parameters (see text), extracted from the fit, are shown in the bottom-right corner of the plot. As can be seen, HEPD-01 provides proton measurements at higher energies with respect to EPHIN and ERNE.

functions are depicted in Figure 5 as blue (Weibull), green (Band) and red (Ellison-Ramaty) curves. The Weibull seems to be the best choice in this case, but the not perfect magnetic connectivity and the long duration of the event itself, together with the intrinsic uncertainties related to the process of event integration, suggest that transport may play a significant role in modifying the source acceleration spectrum. Nevertheless, it is possible that the time-integrated spectrum may still contain traces of the imprint of the acceleration at the solar source (Reames & Ng, 2010). A discussion will be presented in Section 7.

6. Arrival Time Analysis

The propagation of SEP particles from the surface of the Sun—where the flare has happened—to 1 AU depends on the nature of the event itself. If such particles are all accelerated at the same time and from the same region of the Sun, and traverse the same magnetic path-length before being observed, a detector would register a dispersion in their velocities; this means that the onset of an event for higher energy particles would occur before the onset of lower energy ones, see for example Lin et al. (1981); Reames et al. (1985); Krucker et al. (1999). This is particularly true for the GLE under study, where the first arriving particles can be assumed to be almost scatter-free. Following the example in Vainio et al. (2013); Thakur et al. (2013) and using HEPD-01, EPHIN and ERNE proton data, it is possible to build a distribution of these onset times as a function of the variable 1/velocity—see Figure 6. A linear fit provides information on the Solar Particle Release or SPR time (intercept) and the magnetic path-length traversed by the particles (slope). In order to associate the source of acceleration with physical processes at the Sun, such as CME-driven shocks and magnetic reconnection, we compare the SPR time—obtained from the fit—with the time of the type II radio emission, the maximum of the X-ray emission and the first observation of the CME by LASCO/C2, all marked in Figure 6.

7. Discussion and Conclusions

Useful information can be obtained from the SEP/GLE energy spectra observed in the interplanetary space, both for Space Weather purposes (as discussed in Section 1) and for gaining insights into particle acceleration. As a matter of fact, even if transport plays an important role in modifying the spectrum with respect to the one at the source of acceleration, the extended energy spectrum could possibly be somewhat representative of the one at the source. Therefore, we obtained the energy spectrum for the 28 October 2021 SEP/GLE event in the wide energy range 300 keV–250 MeV, by combining the measures from ACE/ULEIS, SOHO/EPHIN, SOHO/ERNE, and HEPD-01. First, we studied the spectral evolution of the SEP proton spectra (Figure 4), measured by HEPD-01 during the early hours of the event, by using a simple power law function, as predicted by the DSA. A gradual softening of the γ index is observed—from ~1.12 to ~2.47—in good agreement with what has been shown in Bruno et al. (2019) for the X8.2 SEP of 10 September 2017, which triggered a GLE. Nevertheless, other

spectral shapes have been proposed in the past, such as the Band function and the Weibull; the last one has been found to be in better agreement with the observed SEP spectrum. In particular, it has been suggested in Laurenza et al. (2015) that the Weibull distribution is the best fit for gradual SEP events, as well as for particle enhancements at interplanetary transient shocks (see also Chiappetta et al., 2021) and shocks at corotating interaction regions. We found that the Weibull functional form reproduces the 28 October 2021 SEP/GLE event spectrum (see Figure 5) better than the alternative proposed functions like Band and Ellison-Ramaty, as can be inferred by a comparison between the reduced χ^2—0.48 for the Weibull, 0.94 for the Band and 1.12 for the Ellison-Ramaty— confirming past results. The Weibull distribution has been also theoretically derived in the framework of stochastic acceleration and associated with acceleration at shock waves (Laurenza et al., 2016; Pallocchia et al., 2017). More specifically, these papers present a theoretical derivation of the Weibull spectrum, involving the effect of stochastic acceleration at shock waves, in case of momentum anomalous diffusion. Thus, the stochastic acceleration of protons in the downstream region of a shock can be an additional mechanism for producing the observed particle energy spectra associated with CME-driven shocks. Indeed, stochastic acceleration in the vicinity of shock waves has been found to be efficient Ostrowski (1994) both in terms of energy budget and acceleration time, due to the presence of high amplitude MHD turbulence. In addition, Schlickeiser et al. (1993) proposed that due to efficient momentum diffusion of particles in the downstream region of the shock, the acceleration is dominated by the second order acceleration mechanism and the particle spectra become flatter than in the original treatment of diffusive shock acceleration. Stochastic acceleration could also act as a re-acceleration of energetic protons by enhanced turbulence in the downstream region of the shock, as proposed by Afanasiev et al. (2014) for relativistic energies in case of GLE events.

We found the following values of the Weibull parameters for the SEP/GLE event under study: $b = 0.28 \pm 0.06$ and $E_0 = 0.034 \pm 0.027$ MeV. The b and E_0 parameters of the Weibull function are indicative of the acceleration efficiency, the former (assuming values between 0 and 1), being related to the rate of the particle energy increase during the confinement around the shock, the latter representing a characteristic energy of a particle after a typical confinement time. In the case of efficient energization, the mean energy E_0 has to be much higher than the typical injection energy. Therefore, in the case of GLE#73, we suggest that the energetic particle population may be accelerated directly out of the ambient coronal material by a turbulent shock, even if its variability, the effect of transport and the presence of seed populations may play a rather important role. Nevertheless, as the Weibull distribution has been derived in the framework of stochastic acceleration, the flare acceleration cannot be excluded.

For what concerns the arrival times of protons—see Figure 6—we have compared the SPR time obtained from the first-degree polynomial fit (1601 UTC $\pm$ 13 min) with both the time of the type II radio emission (1528 UTC), the maximum of the X-ray emission (1535 UTC) and the observation of the CME by LASCO/C2 (1548 UTC). We also have found a magnetic path-length distance traversed by the particles equal to $L = 1.32 \pm 0.24$ AU. It is clear that the initial SPR occurs after the onset times of type II emission, in agreement with what has been found in Reames (2009). Unfortunately, due to the large errors in the parameters of the fit, we can not give a more confident interpretation of the mechanisms that rule this GLE event. However, our findings for the path-length and SPR time are in a good agreement with the results shown in Papaioannou, A. et al. (2022) and obtained using the solar wind speed. It is also important to stress that, thanks to the capabilities of HEPD-01, the Limadou mission has provided some solid SEP measurements in the high-energy portion of the proton spectrum, which could help in better understanding the nature of the acceleration mechanisms at play in SEP events during the forthcoming solar cycle and beyond, as HEPD-01 is still operative and HEPD-02 is in the final stages of integration and it is expected to start taking data in 2023.

Data Availability Statement

HEPD-01 data are available, upon request, at https://limadou.ssdc.asi.it/.

References

Afanasiev, A., Vainio, R., & Kocharov, L. (2014). The effect of stochastic re-acceleration on the energy spectrum of shock-accelerated protons. *The Astrophysical Journal*, *790*(1), 36. https://doi.org/10.1088/0004-637x/790/1/36

Afanasiev, A., Vainio, R., Rouillard, A. P., Battarbee, M., Aran, A., & Zucca, P. (2018). Modelling of proton acceleration in application to a ground level enhancement. *Astronomy and Astrophysics*, *614*, A4. https://doi.org/10.1051/0004-6361/201731343

Ambrosi, G., Bartocci, S., Basara, L., Battiston, R., Burger, W., Campana, D., et al. (2021). The electronics of the high-energy particle detector on board the CSES-01 satellite. *Nuclear Instruments and Methods in Physics Research Section A: Accelerators, Spectrometers, Detectors and Associated Equipment*, *1013*, 165639. https://doi.org/10.1016/j.nima.2021.165639

Ambrosi, G., Bartocci, S., Basara, L., Battiston, R., Burger, W. J., Campana, D., et al. (2020). Beam test calibrations of the HEPD detector on board the China Seismo-Electromagnetic Satellite. *Nuclear Instruments and Methods in Physics Research*, *974*, 164170. https://doi.org/10.1016/j.nima.2020.164170

Aschwanden, M. J. (2002). Particle acceleration and kinematics in solar flares. In *Particle acceleration and kinematics in solar flares* (pp. 1–227). Springer.

Band, D., Matteson, J., Ford, L., Schaefer, B., Palmer, D., Teegarden, B., et al. (1993). BATSE observations of gamma-ray burst spectra. I. Spectral diversity. *The Astrophysical Journal*, *413*, 281. https://doi.org/10.1086/172995

Bartocci, S., Battiston, R., Burger, W. J., Campana, D., Carfora, L., Castellini, G., et al. (2020). Galactic cosmic-ray hydrogen spectra in the 40–250 MeV range measured by the high-energy particle detector (HEPD) on board the CSES-01 Satellite between 2018 and 2020. *The Astrophysical Journal*, *901*(1), 8. https://doi.org/10.3847/1538-4357/abad3e

Berrilli, F., Casolino, M., Del Moro, D., Di Fino, L., Larosa, M., Narici, L., et al. (2014). The relativistic solar particle event of May 17th, 2012 observed on board the International Space Station. *Journal of Space Weather and Space Climate*, *4*, A16. https://doi.org/10.1051/swsc/2014014

Bieber, J. W., Dröge, W., Evenson, P. A., Pyle, R., Ruffolo, D., Pinsook, U., et al. (2002). Energetic particle observations during the 2000 July 14 solar event. *The Astrophysical Journal*, *567*(1), 622–634. https://doi.org/10.1086/338246

Brueckner, G. E., Howard, R. A., Koomen, M. J., Korendyke, C. M., Michels, D. J., Moses, J. D., et al. (1995). The large angle spectroscopic Coronagraph (LASCO). *Solar Physics*, *162*(1–2), 357–402. https://doi.org/10.1007/BF00733434

Bruno, A., Bazilevskaya, G. A., Boezio, M., Christian, E. R., de Nolfo, G. A., Martucci, M., et al. (2018). Solar energetic particle events observed by the PAMELA mission. *The Astrophysical Journal*, *862*(2), 97. https://doi.org/10.3847/1538-4357/aacc26

Bruno, A., Christian, E. R., de Nolfo, G. A., Richardson, I. G., & Ryan, J. M. (2019). Spectral analysis of the September 2017 solar energetic particle events. *Space Weather*, *17*(3), 419–437. https://doi.org/10.1029/2018SW002085

Cane, H. V., McGuire, R. E., & von Rosenvinge, T. T. (1986). Two classes of solar energetic particle events associated with impulsive and long-duration soft X-ray flares. *The Astrophysical Journal*, *301*, 448. https://doi.org/10.1086/163913

Cane, H. V., Mewaldt, R. A., Cohen, C. M. S., & von Rosenvinge, T. T. (2006). Role of flares and shocks in determining solar energetic particle abundances. *Journal of Geophysical Research*, *111*(A6), A06S90. https://doi.org/10.1029/2005JA011071

Cane, H. V., Richardson, I. G., & von Rosenvinge, T. T. (2010). A study of solar energetic particle events of 1997–2006: Their composition and associations. *Journal of Geophysical Research*, *115*(A8), A08101. https://doi.org/10.1029/2009JA014848

Chiappetta, F., Laurenza, M., Lepreti, F., & Consolini, G. (2021). Proton energy spectra of energetic storm particle events and relation with shock parameters and turbulence. *The Astrophysical Journal*, *915*(1), 8. https://doi.org/10.3847/1538-4357/abfe09

Cliver, E. W. (1996). Solar flare gamma-ray emission and energetic particles in space. In R. Ramaty, N. Mandzhavidze, & X.-M. Hua (Eds.), *High energy solar physics* (Vol. *374*, pp. 45–60). https://doi.org/10.1063/1.50980

Cliver, E. W., Kahler, S. W., Shea, M. A., & Smart, D. F. (1982). Injection onsets of 2 GeV protons, 1 MeV electrons, and 100 keV electrons in solar cosmic ray flares. *The Astrophysical Journal*, *260*, 362–370. https://doi.org/10.1086/160261

Damiani, A., Storini, M., Laurenza, M., & Rafanelli, C. (2008). Solar particle effects on minor components of the polar atmosphere. *Annales Geophysicae*, *26*(2), 361–370. https://doi.org/10.5194/angeo-26-361-2008

Dayeh, M., Desai, M., Dwyer, J., Rassoul, H., Mason, G., & Mazur, J. (2009). Composition and spectral properties of the 1 au quiet-time suprathermal ion population during solar cycle 23. *The Astrophysical Journal*, *693*(2), 1588–1600. https://doi.org/10.1088/0004-637x/693/2/1588

Desai, M., & Giacalone, J. (2016). Large gradual solar energetic particle events. *Living Reviews in Solar Physics*, *13*(1), 3. https://doi.org/10.1007/s41116-016-0002-5

Diego, P., & Laurenza, M. (2021). Geomagnetic activity recurrences for predicting the amplitude and shape of solar cycle n. 25. *Journal of Space Weather and Space Climate*, *11*, 52. https://doi.org/10.1051/swsc/2021036

Domingo, V., Fleck, B., & Poland, A. I. (1995). The SOHO mission: An overview. *Solar Physics*, *162*(1–2), 1–37. https://doi.org/10.1007/BF00733425

Dresing, N., Gómez-Herrero, R., Klassen, A., Heber, B., Kartavykh, Y., & Dröge, W. (2012). The large longitudinal spread of solar energetic particles during the 17 January 2010 solar event. *Solar Physics*, *281*(1), 281–300. https://doi.org/10.1007/s11207-012-0049-y

Dröge, W., Kartavykh, Y., Dresing, N., & Klassen, A. (2016). Multi-spacecraft observations and transport modeling of energetic electrons for a series of solar particle events in August 2010. *The Astrophysical Journal*, *826*(2), 134. https://doi.org/10.3847/0004-637x/826/2/134

Ellison, D. C., & Ramaty, R. (1985). Shock acceleration of electrons and ions in solar flares. *The Astrophysical Journal*, *298*, 400–408. https://doi.org/10.1086/163623

Erwan, T., Finlay, C., Beggan, C., Alken, P., Aubert, J., Barrois, O., et al. (2015). International geomagnetic reference field: The 12th generation. *Earth Planets and Space*, *67*(1), 79. https://doi.org/10.1186/s40623-015-0228-9

Frassati, F., Laurenza, M., Bemporad, A., West, M. J., Mancuso, S., Susino, R., et al. (2022). Acceleration of solar energetic particles through CME-driven shock and streamer interaction. *The Astrophysical Journal*, *926*(2), 227. https://doi.org/10.3847/1538-4357/ac460e

Frisch, U., & Sornette, D. (1997). Extreme deviations and applications. *Journal de Physique I*, *7*(9), 1155–1171. https://doi.org/10.1051/jp1:1997114

Georgoulis, M. K., Nindos, A., & Zhang, H. (2019). The source and engine of coronal mass ejections. *Philosophical Transactions of the Royal Society of London, Series A*, *377*(2148), 20180094. https://doi.org/10.1098/rsta.2018.0094

Gopalswamy, N., Mäkelä, P., Yashiro, S., Lara, A., Xie, H., Akiyama, S., & MacDowall, R. J. (2018). Interplanetary type II radio bursts from wind/WAVES and sustained gamma-ray emission from Fermi/LAT: Evidence for shock source. *The Astrophysical Journal Letters*, *868*(2), L19. https://doi.org/10.3847/2041-8213/aaef36

Gopalswamy, N., Xie, H., Yashiro, S., Akiyama, S., Mäkelä, P., & Usoskin, I. G. (2012). Properties of ground level enhancement events and the associated solar eruptions during solar cycle 23. *Space Science Reviews*, *171*(1–4), 23–60. https://doi.org/10.1007/s11214-012-9890-4

Gordon, B. E., Lee, M. A., Möbius, E., & Trattner, K. J. (1999). Coupled hydromagnetic wave excitation and ion acceleration at interplanetary traveling shocks and Earth's bow shock revisited. *Journal of Geophysical Research*, *104*(A12), 28263–28278. https://doi.org/10.1029/1999JA900356

Grimani, C., Boatella, C., Chmeissani, M., Fabi, M., Finetti, N., Lobo, A., & Mateos, I. (2012). Scientific goals achievable with radiation monitor measurements on board gravitational wave interferometers in space. *Journal of Physics: Conference Series*, *363*, 012045. https://doi.org/10.1088/1742-6596/363/1/012045

Jackman, C. H., Deland, M. T., Labow, G. J., Fleming, E. L., Weisenstein, D. K., Ko, M. K. W., et al. (2005). Neutral atmospheric influences of the solar proton events in October–November 2003. *Journal of Geophysical Research*, *110*(A9), A09S27. https://doi.org/10.1029/2004JA010888

Jain, K., Lindsey, C., & Tripathy, S. C. (2021). What is exceptional about solar activity in the early phase of cycle 25? *Research Notes of the American Astronomical Society*, *5*(10), 253. https://doi.org/10.3847/2515-5172/ac3429

Kahler, S. W., Cliver, E. W., Tylka, A. J., & Dietrich, W. F. (2012). A Comparison of Ground Level Event e/p and Fe/O ratios with associated solar flare and CME characteristics. *Space Science Reviews*, *171*(1–4), 121–139. https://doi.org/10.1007/s11214-011-9768-x

Kahler, S. W., Hildner, E., & Van Hollebeke, M. A. I. (1978). Promt solar proton events and coronal mass ejections. *Solar Physics*, *57*(2), 429–443. https://doi.org/10.1007/BF00160116

Kahler, S. W., Kazachenko, M., Lynch, B. J., & Welsch, B. T. (2017). Flare magnetic reconnection fluxes as possible signatures of flare contributions to gradual SEP events. *Journal of Physics: Conference Series*, *900*, 012011. https://doi.org/10.1088/1742-6596/900/1/012011

Kahler, S. W. Jr., Sheeley, N. R., Howard, R. A., Michels, D. J., Koomen, M. J., McGuire, R. E., et al. (1984). Associations between coronal mass ejections and solar energetic proton events. *Journal of Geophysical Research*, *89*(A11), 9683–9694. https://doi.org/10.1029/JA089iA11p09683

Kim, M.-H. Y., Cucinotta, F. A., & Wilson, J. W. (2007). A temporal forecast of radiation environments for future space exploration missions. *Radiation and Environmental Biophysics*, *46*(2), 95–100. https://doi.org/10.1007/s00411-006-0080-1

Kollhoff, A., Kouloumvakos, A., Lario, D., Dresing, N., Gómez-Herrero, R., Rodriguez-Garcia, L., et al. (2021). The first widespread solar energetic particle event observed by solar orbiter on 2020 November 29. *Astronomy & Astrophysics*, *656*, A20. https://doi.org/10.1051/0004-6361/202140937

Kouloumvakos, A., Rouillard, A. P., Share, G. H., Plotnikov, I., Murphy, R., Papaioannou, A., & Wu, Y. (2020). Evidence for a coronal shock wave origin for relativistic protons producing solar gamma-rays and observed by neutron monitors at Earth. *The Astrophysical Journal*, *893*(1), 76. https://doi.org/10.3847/1538-4357/ab8227

Krucker, S., Larson, D. E., Lin, R. P., & Thompson, B. J. (1999). On the origin of impulsive electron events observed at 1 AU. *The Astrophysical Journal*, *519*(2), 864–875. https://doi.org/10.1086/307415

Laitinen, T., Kopp, A., Effenberger, F., Dalla, S., & Marsh, M. S. (2016). Solar energetic particle access to distant longitudes through turbulent field-line meandering. *Astronomy & Astrophysics*, *591*, A18. https://doi.org/10.1051/0004-6361/201527801

Laurenza, M., Alberti, T., Marcucci, M. F., Consolini, G., Jacquey, C., Molendi, S., et al. (2019). Estimation of the particle radiation environment at the L1 point and in near-Earth space. *The Astrophysical Journal*, *873*(2), 112. https://doi.org/10.3847/1538-4357/ab0410

Laurenza, M., Consolini, G., Storini, M., & Damiani, A. (2013). On the spectral shape of SEP events: An extreme value statistics approach. In G. P. Zank (Eds.), *Solar wind 13* (Vol. *1539*, pp. 219–222). https://doi.org/10.1063/1.4811027

Laurenza, M., Consolini, G., Storini, M., & Damiani, A. (2015). The Weibull functional form for SEP event spectra. *Journal of Physics: Conference Series*, *632*, 012066. https://doi.org/10.1088/1742-6596/632/1/012066

Laurenza, M., Consolini, G., Storini, M., Pallocchia, G., & Damiani, A. (2016). The Weibull functional form for the energetic particle spectrum at interplanetary shock waves. *Journal of Physics: Conference Series*, *767*, 012015. https://doi.org/10.1088/1742-6596/767/1/012015

Lee, M. A. (1983). Coupled hydromagnetic wave excitation and ion acceleration at interplanetary traveling shocks. *Journal of Geophysical Research*, *88*(A8), 6109–6120. https://doi.org/10.1029/JA088iA08p06109

Lemen, J. R., Title, A. M., Akin, D. J., Boerner, P. F., Chou, C., Drake, J. F., et al. (2012). The atmospheric imaging assembly (AIA) on the solar dynamics observatory (SDO). *Solar Physics*, *275*(1–2), 17–40. https://doi.org/10.1007/s11207-011-9776-8

Lin, R. P., Potter, D. W., Gurnett, D. A., & Scarf, F. L. (1981). Energetic electrons and plasma waves associated with a solar type III radio burst. *The Astrophysical Journal*, *251*, 364–373. https://doi.org/10.1086/159471

Martucci, M., Bartocci, S., Battiston, R., Campana, D., Carfora, L., Conti, L., et al. (2022). New results on protons inside the South Atlantic Anomaly, at energies between 40–250 MeV in the period 2018–2020, from the CSES-01 satellite mission. *Physical Review D*, *105*(6), 062001. https://doi.org/10.1103/PhysRevD.105.062001

Mason, G. M., Gold, R. E., Krimigis, S. M., Mazur, J. E., Andrews, G. B., Daley, K. A., et al. (1998). The ultra-low-energy isotope spectrometer (ULEIS) for the ACE spacecraft. *Space Science Reviews*, *86*(1/4), 409–448. https://doi.org/10.1023/A:1005079930780

Mavromichalaki, H., Papaioannou, A., Plainaki, C., Sarlanis, C., Souvatzoglou, G., Gerontidou, M., et al. (2011). Applications and usage of the real-time neutron monitor database. *Advances in Space Research*, *47*(12), 2210–2222. https://doi.org/10.1016/j.asr.2010.02.019

McCracken, K. G., Moraal, H., & Stoker, P. H. (2008). Investigation of the multiple-component structure of the 20 January 2005 cosmic ray ground level enhancement. *Journal of Geophysical Research*, *113*(A12), A12101. https://doi.org/10.1029/2007JA012829

Mewaldt, R. A., Looper, M. D., Cohen, C. M. S., Haggerty, D. K., Labrador, A. W., Leske, R. A., et al. (2012). Energy spectra, composition, and other properties of ground-level events during solar cycle 23. *Space Science Reviews*, *171*(1–4), 97–120. https://doi.org/10.1007/s11214-012-9884-2

Miteva, R., Samwel, S. W., Zabunov, S., & Dechev, M. (2020). On the flux saturation of SOHO/ERNE proton events. *Bulgarian Astronomical Journal*, *33*, 99.

Moraal, H., & McCracken, K. G. (2012). The time structure of ground level enhancements in solar cycle 23. *Space Science Reviews*, *171*(1–4), 85–95. https://doi.org/10.1007/s11214-011-9742-7

Müller-Mellin, R., Kunow, H., Fleißner, V., Pehlke, E., Rode, E., Röschmann, N., et al. (1995). COSTEP—comprehensive suprathermal and energetic particle analyser. *Solar Physics*, *162*(1–2), 483–504. https://doi.org/10.1007/BF00733437

Nitta, N. V., Liu, Y., DeRosa, M. L., & Nightingale, R. W. (2012). What are special about ground-level events?. Flares, CMEs, active regions and magnetic field connection. *Space Science Reviews*, *171*(1–4), 61–83. https://doi.org/10.1007/s11214-012-9877-1

Ostrowski, M. (1994). Efficiency of the second-order Fermi acceleration at parallel shock waves. *Astronomy and Astrophysics*, *283*(1), 344–348.

Pallavicini, R., Serio, S., & Vaiana, G. S. (1977). A survey of soft X-ray limb flare images: The relation between their structure in the corona and other physical parameters. *The Astrophysical Journal*, *216*, 108–122. https://doi.org/10.1086/155452

Pallocchia, G., Laurenza, M., & Consolini, G. (2017). On Weibull's spectrum of non-relativistic energetic particles at IP shocks: Observations and theoretical interpretation. *The Astrophysical Journal*, *837*(2), 158. https://doi.org/10.3847/1538-4357/aa633a

Palma, F., Sotgiu, A., Parmentier, A., Martucci, M., Piersanti, M., Bartocci, S., et al. (2021). The August 2018 geomagnetic storm observed by the high-energy particle detector on board the CSES-01 satellite. *Applied Sciences*, *11*(12), 5680. https://doi.org/10.3390/app11125680

Papaioannou, A., Kouloumvakos, A., Mishev, A., Vainio, R., Usoskin, I., Herbst, K., et al. (2022). The first ground-level enhancement of solar cycle 25 on 28 october 2021. *Astronomy & Astrophysics*, *660*, L5. https://doi.org/10.1051/0004-6361/202142855

Penza, V., Berrilli, F., Bertello, L., Cantoresi, M., & Criscuoli, S. (2021). Prediction of sunspot and plage coverage for solar cycle 25. *The Astrophysical Journal Letters*, *922*(1), L12. https://doi.org/10.3847/2041-8213/ac3663

Pérez-Peraza, J., Márquez-Adame, J. C., Miroshnichenko, L., & Velasco-Herrera, V. (2018). Source energy spectrum of the 17 May 2012 GLE. *Journal of Geophysical Research: Space Physics*, *123*(5), 3262–3272. https://doi.org/10.1002/2017JA025030

Pesnell, W. D., Thompson, B. J., & Chamberlin, P. (2011). The solar dynamics observatory (SDO). In *The solar dynamics observatory* (pp. 3–15). Springer.

Picozza, P., Battiston, R., Ambrosi, G., Bartocci, S., Basara, L., Burger, W. J., et al. (2019). Scientific goals and in-orbit performance of the high-energy particle detector on board the CSES. *Astrophysical Journal Supplements*, *243*(1), 16. https://doi.org/10.3847/1538-4365/ab276c

Piersanti, M., Del Moro, D., Parmentier, A., Martucci, M., Palma, F., Sotgiu, A., et al. (2022). On the magnetosphere-ionosphere coupling during the May 2021 geomagnetic storm. *Space Weather*, *20*(6), e2021SW003016. https://doi.org/10.1029/2021SW003016

Poluianov, S. V., Usoskin, I. G., Mishev, A. L., Shea, M. A., & Smart, D. F. (2017). GLE and sub-GLE redefinition in the light of high-altitude polar neutron monitors. *Solar Physics*, *292*(11), 176. https://doi.org/10.1007/s11207-017-1202-4

Reames, D. V. (1999). Particle acceleration at the sun and in the heliosphere. *Space Science Reviews*, *90*(3), 413–491. https://doi.org/10.1023/a:1005105831781

Reames, D. V. (2009). Solar energetic-particle release times in historic ground-level events. *The Astrophysical Journal*, *706*(1), 844–850. https://doi.org/10.1088/0004-637x/706/1/844

Reames, D. V., & Ng, C. K. (2010). Streaming-Limited intensities of solar energetic particles on the intensity plateau. *The Astrophysical Journal*, *723*(2), 1286–1293. https://doi.org/10.1088/0004-637x/723/2/1286

Reames, D. V., von Rosenvinge, T. T., & Lin, R. P. (1985). Solar He-3-rich events and nonrelativistic electron events—A new association. *The Astrophysical Journal*, *292*, 716–724. https://doi.org/10.1086/163203

Richardson, I. G., von Rosenvinge, T. T., Cane, H. V., Christian, E. R., Cohen, C. M. S., Labrador, A. W., et al. (2014). 25 MeV proton events observed by the high energy telescopes on the STEREO A and B spacecraft and/or at Earth during the first ∼ seven years of the STEREO mission. *Solar Physics*, *289*(8), 3059–3107. https://doi.org/10.1007/s11207-014-0524-8

Rouillard, A., Sheeley, N., Cooper, T., Davies, J., Lavraud, B., Kilpua, E., et al. (2011). The solar origin of small interplanetary transients. *The Astrophysical Journal*, *734*(1), 7. https://doi.org/10.1088/0004-637x/734/1/7

Rouillard, A. P., Odstřcil, D., Sheeley, N. R., Tylka, A., Vourlidas, A., Mason, G., et al. (2011). Interpreting the properties of solar energetic particle events by using combined imaging and modeling of interplanetary shocks. *The Astrophysical Journal*, *735*(1), 7. https://doi.org/10.1088/0004-637X/735/1/7

Rouillard, A. P., Plotnikov, I., Pinto, R. F., Tirole, M., Lavarra, M., Zucca, P., et al. (2016). Deriving the properties of coronal pressure fronts in 3D: Application to the 2012 May 17 ground level enhancement. *The Astrophysical Journal*, *833*(1), 45. https://doi.org/10.3847/1538-4357/833/1/45

Schlickeiser, R., Campeanu, A., & Lerche, L. (1993). Stochastic particle acceleration at parallel astrophysical shock waves. *Astronomy and Astrophysics*, *276*, 614.

Shen, X., Zhang, X., Yuan, S., Wang, L., Cao, J., Huang, J., et al. (2018). The state-of-the-art of the China Seismo-Electromagnetic Satellite mission. *Science in China E: Technological Sciences*, *61*(5), 634–642. https://doi.org/10.1007/s11431-018-9242-0

Sotgiu, A., De Donato, C., Fornaro, C., Tassa, S., Scannavini, M., Iannaccio, D., et al. (2020). Control and data acquisition software of the high-energy particle detector on board the China Seismo-Electromagnetic Satellite Space Mission. Software: Practice and experience (Vol. *1–22*). https://doi.org/10.1002/spe.2947

Stephens, G. K., Morrison, D., Barnes, R. J., Potter, M., & Schaefer, R. K. (2017). Up-to-date geomagnetic coordinate transforms with AACGM. *AGU fall meeting abstracts*, *2017*, SM13C–2395.

Thakur, N., Boezio, M., Bravar, U., Christian, E. R., de Nolfo, G. A., Martucci, M., et al. (2013). Study of 2012 May 17 GLE with PAMELA. In *AGU spring meeting abstracts* (Vol. *2013*, SH33B-06).

Torsti, J. J., Valtonen, E., Lumme, M., Peltonen, J., Eronen, T., Kelhä, V., & Leppälä, K. (1991). Scientific performance of ERNE sensors. *Advances in Space Research*, *11*(1), 401–404. https://doi.org/10.1016/0273-1177(91)90138-A

Tsyganenko, N. A. (1995). Modeling the Earth's magnetospheric magnetic field confined within a realistic magnetopause. *Journal of Geophysical Research*, *100*(A4), 5599–5612. https://doi.org/10.1029/94JA03193

Tylka, A. J., Cohen, C. M. S., Dietrich, W. F., Lee, M. A., Maclennan, C. G., Mewaldt, R. A., et al. (2005). Shock geometry, seed populations, and the origin of variable elemental composition at high energies in large gradual solar particle events. *The Astrophysical Journal*, *625*(1), 474–495. https://doi.org/10.1086/429384

Tylka, A. J., Dietrich, W., & Atwell, W. (2010). Band function representations of solar proton spectra in ground-level events. *38th COSPAR Scientific Assembly*, *38*, 4.

Vainio, R., Raukunen, O., Tylka, A. J., Dietrich, W. F., & Afanasiev, A. (2017). Why is solar cycle 24 an inefficient producer of high-energy particle events? *Astronomy and Astrophysics*, *604*, A47. https://doi.org/10.1051/0004-6361/201730547

Vainio, R., Valtonen, E., Heber, B., Malandraki, O. E., Papaioannou, A., Klein, K.-L., et al. (2013). The first SEPServer event catalogue ~68-MeV solar proton events observed at 1 AU in 1996–2010. *Journal of Space Weather and Space Climate*, 3, A12. https://doi.org/10.1051/swsc/2013030

Vashenyuk, E. V., Balabin, Y. V., & Gvozdevsky, B. B. (2011). Features of relativistic solar proton spectra derived from ground level enhancement events (GLE) modeling. *Astrophysics and Space Sciences Transactions*, *7*(4), 459–463. https://doi.org/10.5194/astra-7-459-2011

Vashenyuk, E. V., Balabin, Y. V., Perez-Peraza, J., Gallegos-Cruz, A., & Miroshnichenko, L. I. (2006). Some features of the sources of relativistic particles at the Sun in the solar cycles 21 23. *Advances in Space Research*, *38*(3), 411–417. https://doi.org/10.1016/j.asr.2005.05.012

Wild, J. P., Smerd, S. F., & Weiss, A. A. (1963). Solar bursts. *Annual Review of Astronomics andAstrophysics*, 1, 291–366. https://doi.org/10.1146/annurev.aa.01.090163.001451

Xapsos, M. A., Barth, J. L., Stassinopoulos, E. G., Messenger, S. R., Walters, R. J., Summers, G. P., & Burke, E. A. (2000). Characterizing solar proton energy spectra for radiation effects applications. *IEEE Transactions on Nuclear Science*, *47*(6), 2218–2223. https://doi.org/10.1109/23.903756

Zhang, J., Temmer, M., Gopalswamy, N., Malandraki, O., Nitta, N. V., Patsourakos, S., et al. (2021). Earth-affecting solar transients: A review of progresses in solar cycle 24. *Progress in Earth and Planetary Science*, *8*(1), 56. https://doi.org/10.1186/s40645-021-00426-7

Zhao, L. L., Zank, G. P., Khabarova, O., Du, S., Chen, Y., Adhikari, L., & Hu, Q. (2018). An unusual energetic particle flux enhancement associated with solar wind magnetic island dynamics. *The Astrophysical Journal Letters*, *864*(2), L34. https://doi.org/10.3847/2041-8213/aaddf6

Zhao, L. L., & Zhang, H. (2016). Transient galactic cosmic-ray modulation during solar cycle 24: A comparative study of two prominent Forbush decrease events, *827*(1), 13. https://doi.org/10.3847/0004-637X/827/1/13